Differential gene expression in cells with different p53 mutations identifies genome-wide p53 targets and shows distinct modulation of cellular pathways in response to DNA damage

Patricia Eror Barnes[1]*, Maria Jose de la Concha[1]*, Kioko Mwikali[2], Bee Ling Ng[3], Hannes Ponstingl[4] and Alena Pance[1#]

1) School of Life and Medical Science, University of Hertfordshire, UK
2) KEMRI-Wellcome, Kilifi, Kenya
3) Flow Cytometry Centre, Wellcome Sanger Institute, UK
4) Human Genetics, Wellcome Sanger Institute, UK
* Contributed equally
# Corresponding author: a.pance@herts.ac.uk

ABSTRACT

The fundamental transcription factor p53 regulates cellular processes and integrates signals of cellular stress, triggering a coordinated response to ensure survival of cells restored to healthy function and programmed death of those that couldn't be repaired. Unsurprisingly, this is one of the most mutated genes in human cancers, with most changes occurring in the DNA-binding domain of the protein. In this work, we take a genome-wide approach and use available resources to identify high confidence p53-target genes, that we examine in three breast cancer cell lines with different p53 status, wild type (MCF-7) and different mutations in the DNA-binding domain (MDA-MB231, T47D). Comparison of p53-targets expression in response to DNA damage by RNAseq and cellular assays reveals that MDA-MB231 have a severely impaired p53-dependent pathway functionality while T47D are much less affected. MDA-MB231 are more resistant to DNA damage yet unable to repair and able to override cell cycle arrest leading to survival while T47D are sensitive only to high dose and exposure to genotoxic agents. This data shows the variability of effects of different p53 mutations and highlight the importance of understanding the mechanisms of p53 in the context of genotoxicity-based treatment.

INTRODUCTION

Cell behaviour and function quickly adapt to environmental cues, with changes triggering a molecular response leading to cell activity, survival or death. The response to insults causing cellular damage such as hypoxia, nutrient deprivation or DNA damage, pivots around p53. The *TP53* gene codes for a tumour suppressor protein acting as a transcription factor that regulates subsets of genes involved in the modulation of the cell cycle, DNA repair and cell fate[1–4]. Thus p53 protects the genome by allowing the cell to repair itself and triggering cell death if repair is not possible. It is not surprising that *TP53* is the most frequently mutated gene in cancer, and breast cancer is no exception. As the highest cause of female mortality[5], much effort has been devoted to finding novel approaches to treat this disease. However, chemo and radiotherapy remain as the mainstream treatment[6], aiming to cause cell death by damaging the DNA and cellular structures. DNA damage, and particularly double-strand breaks (DSB), trigger a cellular response that pivots around p53, the outcomes of which change dramatically if there are mutations that affect functionality of the protein.

Under normal circumstances, p53 is maintained at very low levels due to its thermodynamic instability and short half-life, prompted by constant marking for degradation by MDM2. It is generally present in an inactive state with inefficient DNA binding resulting from rapid unfolding of the core domain at body temperature[7]. Insults such as DNA damage rapidly increase the levels of p53 by MDM2 degradation and the protein is activated and stabilised through post-translational modifications, binding DNA motifs with a specific sequence as a tetrameric

transcription factor[8]. The active protein induces a cellular programme of proteins that will halt cell cycle progression, facilitate DNA damage repair and if it fails, trigger apoptosis. Many of the effector genes are induced directly by p53 binding to their promoters but others are regulated indirectly through the activity of some of the prominent targets, such as *CDKN1A* (p21)[9].

Most mutations in *TP53* occur in the DNA-binding domain (DBD)[10] causing structural changes likely to impact the stability and function of the protein. However, it has been shown that different mutations, can affect p53 function differently either by modifying DNA binding efficiency or modulating interactions with other proteins[11]. Given the fundamental role of p53 and the relevance of mutations in this protein for disease, in particular cancer, it is important to understand its regulatory landscape, its mechanisms and the precise effect of mutations on the functionality of the protein.

In this work, a comprehensive list of direct p53 target genes is generated in order to study p53 function in three human breast cancer cell lines with diverse p53 status. The identified genes are mapped to the cellular pathways modulated by p53 and their expression is examined in cell lines with wild type (WT, MCF-7) and mutated (R280K MDA-MB231 and L194F T47D) p53. Functionality of p53 in these cell lines is assessed exposing the cells to DSB DNA damage.

METHODS

Cell culture

Breast cancer cell lines MCF-7. MDA-MB231 and T47D were maintained in Dulbecco's modified Eagle's medium high glucose (GIBCO) supplemented with 10% foetal calf serum (Fisher Scientific), 2% glutamine (GIBCO) and 1% penicillin/streptomycin (Sigma/Merck) and cultured at 37^{0}C in 5% CO_2. DSB were induced with 4-nitroquinoline 1-oxide (4NQO) (Sigma/Merck).

RNA extraction and sequencing

Cells were treated with 1μM and 10μM 4NQO for 6 hours and total RNA was extracted with Isolate II RNA mini kit (Bioline) following the manufacturer's instructions. Ribominus rRNA depletion kit (ThermoFisher) was used enrichment of messenger RNA. RNA quantification and quality was assessed using Bioanalyzer Pico RNA chips and cDNA were synthesised using Superscript III reverse transcriptase (Invitrogen) following the manufacturer's instructions. cDNA libraries were prepared with NEBNext Ultra II DNA library Prep Kit (New England Biolabs) following the kit protocol and sequenced on Illumina NovaSeq within the Wellcome Sanger pipelines.

MTT assay

Cells were seeded in 96 well plates at 5000 cells per well and left to attach over-night. 24-hour post-seeding, 4NQO was added at 1μM or 10μM for 2 hours or 24 hours. Cells were either measured for viability with an MTT assay or washed with PBS (GIBCO), replacing fresh medium for 24 hours of recovery time and cell viability was measured. Twenty μl of 5mg/ml MTT (3-(4,5-dimethylthiazol-2-yl)-2,5-diphenyltetrazolium bromide) were added per well and incubated at 37^{0}C for 3 hours to form formazan crystals. The reagent and media were removed, and the formazan crystals were then solubilised in 70% ethanol for 30 minutes. Absorbance was measured at 570nM in a plate reader. Absorbance of 4 to 6 replicates was averaged and normalised to controls.

Flow cytometry

Cells were seeded in 6 well plates and left to attach over-night. After treatment with 4NQO, the cells were carefully lifted off the plates by trypsinisation and processed depending on the downstream protocol. Samples were measured on a BD LSR Fortessa™ cell analyser (BD Biosciences).

Cell death assessment: live cells were stained for detection of apoptosis with Hoechst-33342 (excitation/emission: 352/454nm) and necrosis with Propidium Iodide (excitation/emission: 535/615nm). Briefly, cells were resuspended in cold PBS containing 0.5μg/ml Hoechst-33342 and 0.1μg/ml and analysed by flow cytometry. The gating strategy is shown in Supplementary Figure 1: the cell population was chosen on SSC-A/FSC-A eliminating debris (A), from this population doublets were excluded using FSC-W/FSC-A (B) and the singlets population was examined using the 561nm laser 610/20 filter for PI and the 405 laser 450/50 filter for Hoechst-33342. Analysis of unstained, single stained and untreated cells was used to establish the quadrant gates (C), which allowed quantification of the apoptotic cells (high intensity HO staining) in the bottom right quadrant, and the necrotic cells (positive for PI) in the top two quadrants (D). High intensity HO staining reflects nuclear condensation characteristic of apoptosis, while cells positive for PI have compromised membranes, which correspond to necrosis.

Fig. S1

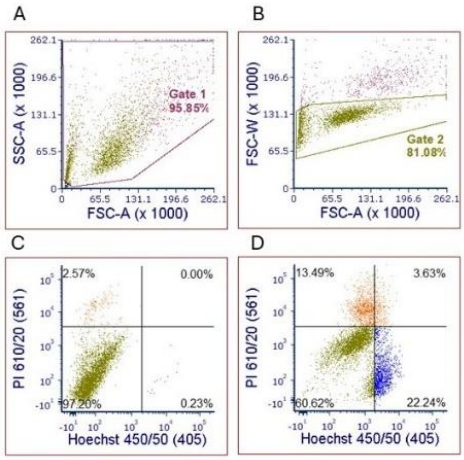

Cell cycle analysis: cells were recovered in cold ethanol (70% in PBS) and fixed over-night at 4^0C. Samples were then centrifuged at 290xg for 5 minutes. The ethanol was discarded, cells were washed 1x with PBS and resuspended in the staining solution: PBS with tritonX-100 (0.1%), RNAse A (SIGMA R6513) (50µg/ml) and Propidium Iodide (25µg/ml). The samples were left staining over-night at 4^0C and analysed the following day using the 561nm laser 610/20 filter on a linear scale. The gating strategy for the cell cycle is shown in Supplementary Figure 2. As above, debris is eliminated from analysis on SSC-A/FSC-A (A) and doublets excluded on PI-W/PI-A (B). The resulting population was analysed for PI fluorescence and the cell cycle phases observed and quantified in a histogram (C) according to intensity reflecting G1 (2n), S (duplicating DNA) and G2/M (4n).

Fig. S2

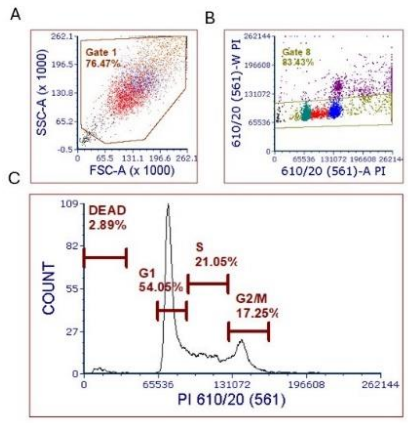

STATISTICAL ANALYSIS

Significance of the differences in cell behaviour detected with the different techniques was assessed by an unpaired two two-tailed distribution T-test.

RESULTS

A comprehensive list of direct p53 target genes shows differences in expression in resting cells with different p53 status

Three breast cancer cell lines with distinct characteristics are used to explore the functionality of p53-regulated cellular processes (Table I). The MCF-7 cell line expresses a wild type (WT) *TP53* while MDA-MB231 and T47D present mutations in the p53 DBD. The mutations are located in different regions of the DBD, affecting different amino acids: MDA-MB231 R280K and T47D L194F, without great impact on p53 expression (Fig.1A). The overall p53 activity in the three cell lines in resting state was calculated using a univariate linear model and the progeny p53 markers (Fig. 1B). This analysis confirmed that p53 activity is severely reduced in the MDA-MB231 line while in T47D activity is affected to a lesser extent, compared to the WT p53 in MCF-7. Because they influence p53-regulated processes, it is important to note that the *BRCA* genes are WT and expressed at similar levels in all three cell lines (Fig. 1A).

Table I. Characteristics of the breast cancer cell lines MCF-7, MDA-MB231 and T47D. *Information obtained from ATCC, Cellosaurus[12] and Cosmic[13].*

	Tumor Type	MOLECULAR CLASSIFICATION		RECEPTOR CHARACTERISTICS						
Cell Line		General Subtype	Subgroup	ER (*ESR1*)	PR (*PGR*)	HER2 (*ERBB2*)	*EGFR*	p53 (*TP53*)	*BRCA1*	*BRCA2*
MCF7	AC	ER+	Luminal A	+	+	++	-	WT	WT	WT
MDA-MB-231	AC	TNBC	Basal B	-	-	+	+	R280K	WT	WT
T47D	DC	ER+	Luminal A	+	++	++	-	L194F	WT	WT

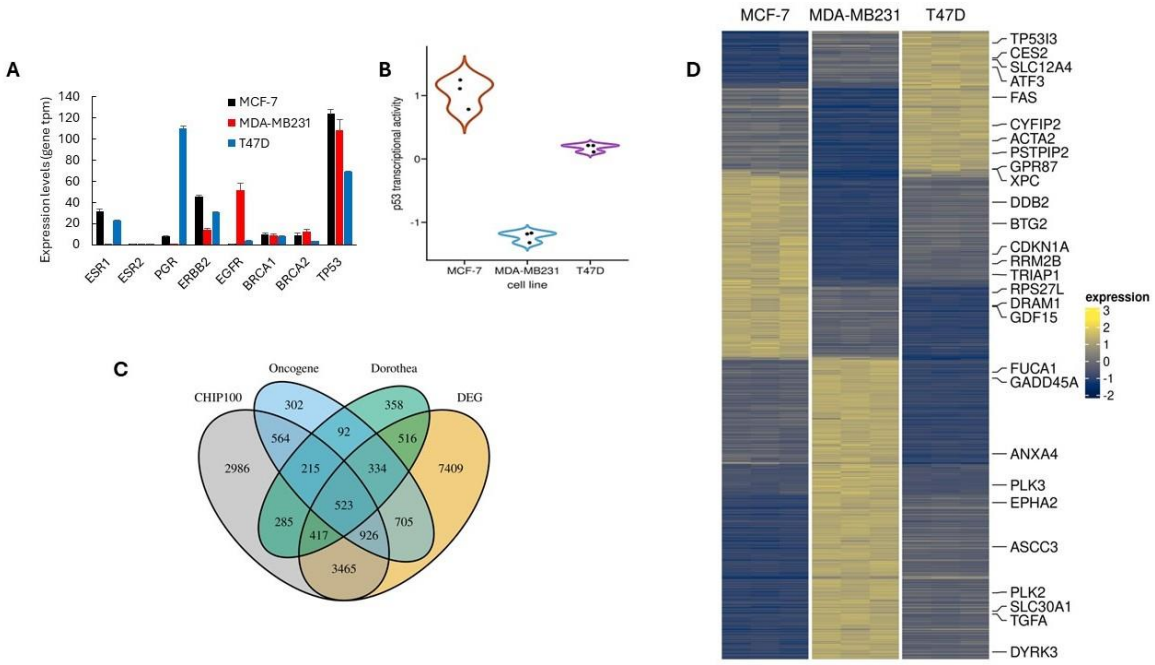

Figure 1. Characteristics and p53 target identification in the breast cancer cell lines. A: *expression levels of breast cancer relevant genes in the cell lines studied, detected by RNAseq, normalised gene tpm data.* ***B:*** *estimation of p53 activity in resting cells, using a univariate linear model and p53 targets.* ***C:*** *Venn diagram of putative direct p53 target genes identified in different data sets, overlapped with differentially expressed genes in the three cell lines.* ***D:*** *Heatmap of high confidence p53 target genes differentially expressed in the three cell lines. DEG found in at least two p53 target data bases.*

In order to understand the regulatory landscape of p53, a comprehensive list of high confidence direct target genes was generated, using several databases available. Genome-wide p53 DNA binding data was obtained from the ChIP-Atlas data base[14], extracting peaks 1Kb around the transcription start sites (TSS) of genes for all breast lines and tissues. Peaks with a minimum binding score of 100 yielded a list

of 9382 potential target genes. This large list was compared with a list of 3661 genes regulated and bound by p53 from an exhaustive study published in 2017 using all existing data at the time[15] and a curated list of 2740 potential targets of varying confidence from the DoRothEA regulon site[16]. These lists revealed a substantial but not complete overlap of the potential p53 target genes identified. Thus, 1440 of the DoRothEA list also show p53 binding in the ChIP-Atlas, which also contained 2228 genes from the study by Fischer[15].

To reconcile the identification of p53 targets, we used the diverse p53 status in the three cell lines and based our approach on the premise that this would cause a difference in expression of the genes directly regulated by p53 in these cell lines. An unbiased analysis was performed by overlapping differentially expressed genes (DEG) in the three cell lines with the lists of target genes identified in the different sources described above (Fig. 1C, Supplementary data). From this comparison, DEG present in at least two of the databases used were compiled in a list of 2203 high confidence direct p53 target genes and their expression pattern in resting state is shown in Figure 1D.

The functionality of p53-dependent cellular processes is affected by p53 status in resting conditions

The list of p53 target genes was used to explore the regulation of cellular pathways in cells with different p53 activity. The Reactome resource[17] (https://reactome.org) pathway database was used to perform a gene set enrichment analysis (GSEA) and compare pathway expression between the cell lines (Fig. 2A, Supplementary data). Interestingly, among the most relevant cellular processes in cancer, DNA repair and cell cycle checkpoint control appear to be downregulated in MDA-MB231 while mitosis and programmed cell death seem to be upregulated in this cell line compared to MCF-7 but downregulated in T47D.

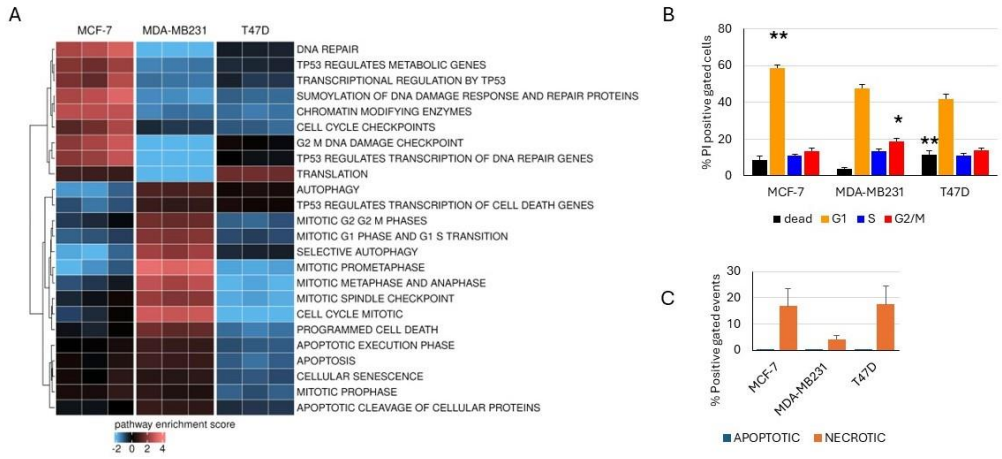

Figure 2. expression and functionality of p53-dependent cellular pathways. A: *heatmap of GSEA for expression of p53 relevant pathways according to the Reactome data base.* ***B:*** *Cell cycle flow cytometric quantification of live cells stained with PI. The gating strategy to determine cell cycle phases is illustrated in the methods section. G1 is significantly higher in MCF-7 compared to MDA-MB231 and T47D (**P<.001), G2/M is higher in MDA-MB231 compared to MCF-7 and T47D (*P<.05), proportion of dead cells is higher in T47D compared to MDA-MB231 (**P<.001) (Average and SEM of 4 experiments).* ***C:*** *cell death analysis in steady state using Hoechst33342 to detect apoptotic cells and Propidium Iodide to quantify Necrotic cell proportions in the resting cell populations. Gating strategy as shown in the methods section (Average and SEM of 4 experiments).*

Consistent with the pathway GSEA, evaluation of the cell cycle by flow cytometry showed that the proportion of cells in G2/M phase is significantly higher in MDA-MB231 compared to the other cell lines, while MCF-7 show a significantly higher proportion of cells in G1 than the others in steady state (Fig. 3B).

The cell cycle assays showed lower levels of cell death in MDA-MB231 and higher in T47D, with a significant difference between these two cell lines (Fig. 2B). Therefore, cell death was examined in more detail, staining live cells with Hoechst33342 (HO) and Propidium Iodide (PI) to detect apoptosis and necrosis respectively. This assessment revealed no apoptosis spontaneously happening in the cells and the death detected in steady state is due to necrosis (Fig. 2C). Levels of death are lower in MDA-MB231 cells than the other lines, though these differences are not statistically significant because of the high variability in cell death in resting cells as these assays are performed with live cells.

The response to double strand break DNA damage is differently affected by distinct mutations in p53

Having detected differences in the expression of p53 target genes in resting conditions, the functionality of p53 was investigated by inducing double strand DNA breaks (DSB) with 4-nitroquinoline 1-oxide (4NQO) and assessing the response to DNA damage. The effect of two concentrations (1 and 10μM) and two exposure times (2h and 24h) was first examined on cell viability using MTT assays (Fig. 3A). MCF-7 cells showed higher sensitivity to long term exposure, while MDA-MB231 were overall more sensitive, particularly to high concentration (10μM at 2h (P<.05) and 24h (P<.005) and T47D had a variable response with little sensitivity to 4NQO. Comparison of the cell lines revealed that cell density of MDA-MB231 to short-term exposure was significantly reduced compared to MCF-7 irrespective of drug concentration (P<.05). The long-term viability of the cells surviving the treatment was tested by restoring fresh medium and allowing recovery for 24 hours (Fig. 3B). Overall, cell recovery was lowest in MCF-7 cells, MDA-MB231 recovered well after short exposure but struggled after prolonged exposure at both concentrations, while T47D seemed most sensitive to the high concentration of 4NQO. Nevertheless, none of the tendencies observed were statistically significant. The effect of two concentrations of 4NQO on gene expression of DEG p53 target genes was examined by RNAseq and the expression patten of genes associated with the DNA repair pathway by Reactome is shown in Figure 3C. The clear differences between the cell lines reflect variation in p53 activity, though subsets of genes involved in this pathway are clearly expressed in all the cell lines.

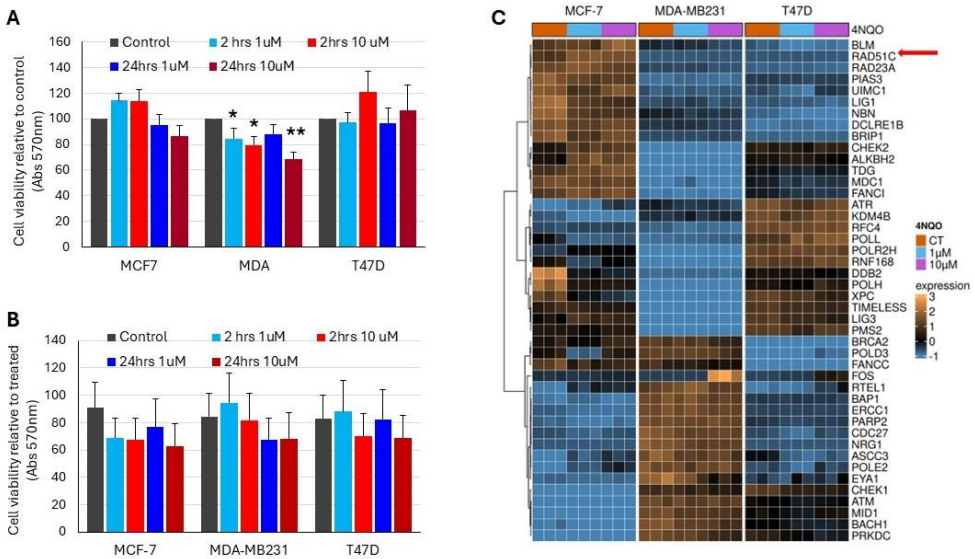

Figure 3. Cell response to DNA damage. *The effect of DSB in the DNA by 4NQO (1μM and 10μM) was analysed by RNAseq and MTTA.* ***A:*** *cell viability after treatment with 4NQO at the both concentrations for 2h and 24 h was assessed by MTTA (SEM on 6 experiments, *P<.05; **P<.005).* ***B:*** *cell viability of surviving cells after treatment allowed to recover in fresh complete medium for 24 h assessed by MTTA (SEM of 6 experiments).* ***C:*** *heatmap of DEG p53 target genes associated with the DNA repair pathway by Reactome.*

Cell cycle status upon DNA damage was analysed by quantifying the proportions of cells at each phase of the cell cycle, as described in the previous section. The main effect of DSB DNA damage was a decrease in G1 with significant differences in the three cell lines (MCF-7 vs MDA-MB231 and T47D P<.05 and MDA-MB231 vs T47D P<.001) upon short exposure to high concentration of 4NQO (Fig. 4A). The most evident changes are increases in cell death after prolonged exposure to DNA damage in MCF-7, while in MDA-MB231 the proportion of dead cells remains fairly constant. T47D cells appear more sensitive to DNA damage, responding with an increase in cell death unrelated to exposure time but directly proportional to the concentration of 4NQO (Fig. 4A).

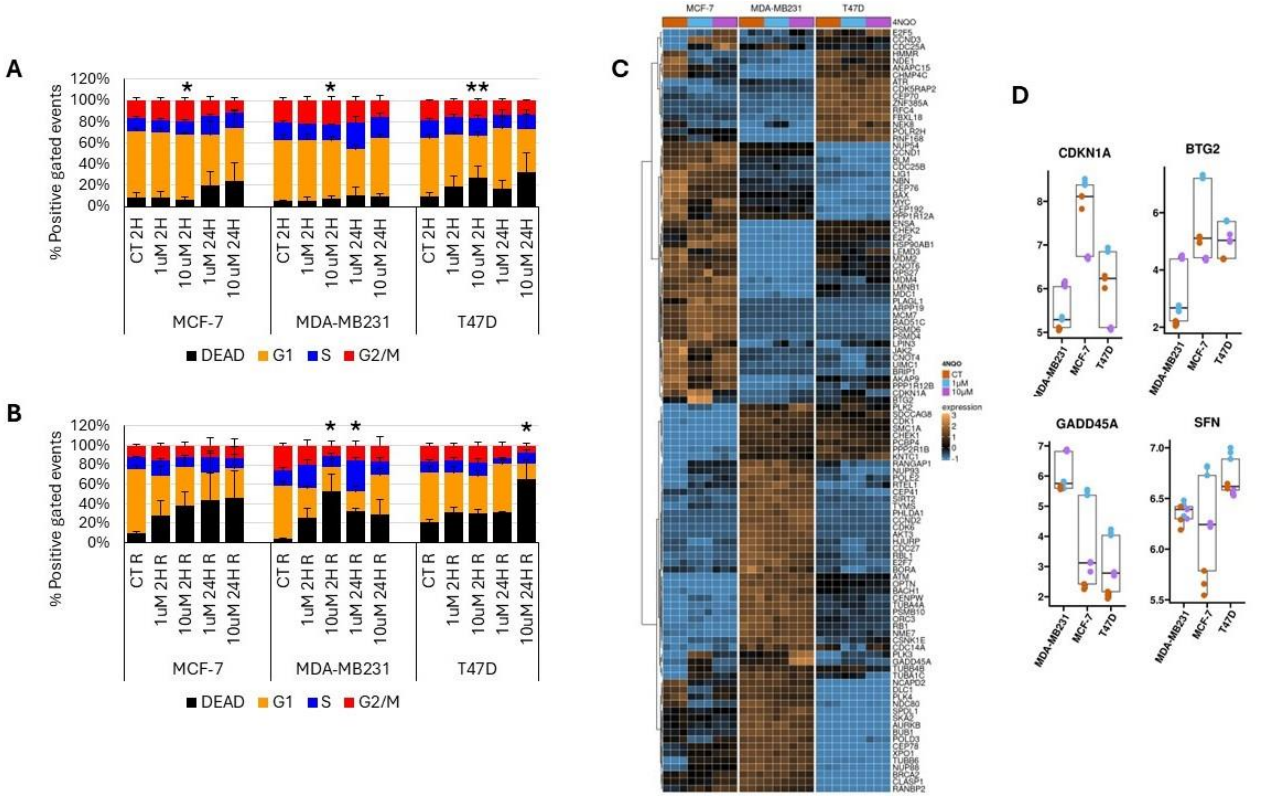

Figure 4. Effect of DSB DNA damage on the cell cycle. *The effect of DNA DSB by 4NQO (1μM and 10μM) for 2h and 24h was analysed by staining with PI.* ***A:*** *the proportion of cells in each phase of the cell cycle was quantified after treatment (Average and SEM of 4 experiments *P<.05, **P<.001).* ***B:*** *cell cycle phases after 24 hours recovery from treatment in each condition (Average and SEM, *P<.05).* ***C:*** *heatmap of DEG p53 target genes assigned to the cell cycle regulation pathway by Reactome.* ***D:*** *overall activity estimation in treated and untreated cells of the indicated genes.*

Restoring of the cell cycle was examined after 24-hour recovery in fresh medium (Fig.4B). Overall, higher levels of death were seen in all cell lines except T47D which only showed a major increase in the harshest condition. The high cell death levels were mirrored by a decrease in G1, most significant in MDA-MB231 treated with 10μM 4NQO for 2h and 1μM for 24h and significant in T47D in the harshest condition (P<.05) compared to their respective controls. Higher levels of S phase were observed in MCF-7 cell recovering from 24h of 1μM 4NQO and this effect is exacerbated in MDA-MB231 while not at all observed in T47D. The G2/M phase decreased in MDA-MB231 but not in the other cell lines, apart from the harshest condition in T47D (Fig. 4B). These results indicate that the T47D cell line is able to restore their cell cycle more effectively than the others after short exposure and low concentration of 4NQO. Expression of cell cycle DEG p53 target genes is visualised in Figure 4C, in a much more complex heatmap because of the high number of genes controlled by p53 within this pathway. As with the DNA repair genes, there are marked differences between the cell lines with some overlap and clear expression of subsets of genes involved in cell cycle control. Notably, while *CDKN1A* and *BGT2* are downregulated in MDA-MB231, *GADD45A* and *SFN* are overexpressed and induced in response to DSB (Fig. 4D).

A closer examination of cell death induced by DNA damage was performed to assess levels of apoptosis and necrosis (Fig. 5A). No significant increase was observed after 2 hours of 1μM 4NQO in any of the cell lines and 24h treatment only induced necrosis in MDA-MB231 (P<.05) compared to their respective controls. In contrast 10μM induced significantly high levels of apoptosis in all cell lines (P<.01) after 2 hours compared to controls and this was reflected in a decrease of live cells. Apoptosis levels were significantly higher than controls on long-term exposure to 10μM in all cell lines (P<.05) while necrosis was significantly higher in MDA-B231 in this condition (P<.01). Comparisons of the cell lines showed a significant increase in necrosis by 10μM 4NQO at both times compared to MCF-7 (P<.05). Comparison of the expression pattern of apoptotic genes identified as DEG and p53TG in a heatmap (Fig. 5B) shows marked differences and little overlap between the cell lines. A large subset of these genes is overexpressed in MDA-MB231, that includes anti-apoptotic genes (*TNFRSF10D, BIRC3*). In fact, some of the genes in the p53 regulatory loop are also differentially expressed and their response to DNA damage varies, such as *MDM2*, which is downregulated in MCF-7 and T47D upon treatment with 4NQO while it is silenced in MDA-MB231. *Chek2* is also silenced in MDA-MB231 but *ATM* and *Chek1* are overexpressed in this cell line (Fig. 5C).

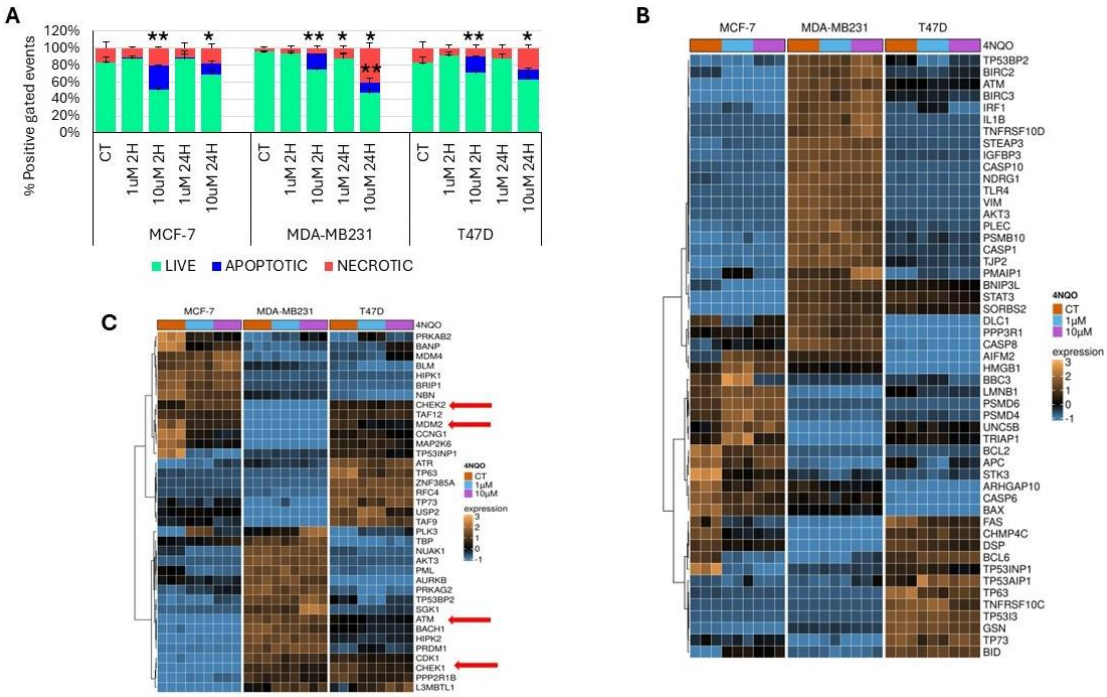

Figure 5. Cell death response to DSB DNA damage. A: *Live cells treated with 4NQO (1μM and 10μM) for 2h and 24h were assessed for apoptosis and necrosis staining with Hoechst33342 and Propidium Iodide respectively, and quantified by flow cytometry (Average and SEM of 4 experiments (*P<.05, **P<.01).* ***B:*** *heatmap of DEG p53 target genes involved in cell death according to Reactome.* ***C:*** *DEG and p53 target genes part of the p53 regulatory feedback pathway as identified by Reactome, red arrows highlight critical genes in this pathway.*

DISCUSSION

As a transcription factor, p53 binds to specific DNA sequences in the promoters of the genes it regulates, yet the task of identifying its direct target genes is in no way trivial. On one hand, its wide and fundamental regulatory function translates in a high number of responsive genes but many of them are indirectly modulated by 'intermediary' proteins induced by p53. Therefore, it is imperative to correlate gene expression with p53 promoter binding, however despite the continuous improvement of technologies such as ChIP-seq and increase in the number of studies reported, this is rather difficult. The lability and short half-life of p53, mean that binding to promoters might be difficult to detect, inducing great variability between studies. Various treatments are used to activate and stabilise p53 on the DNA to increase effectiveness of peak calling. However, this could skew the results because different treatments might lead to distinct DNA binding. Furthermore, published studies use different cell lines, some of which have mutations in *TP53*, which can affect DNA binding and lead to a different profile. Aspects of the protocol used such as the specific antibody, the stringency of the immunoprecipitation washes, the shearing of the chromatin and the threshold for peak calling will have a profound impact on p53 peak detection on genomic DNA. The overlap between the sources of data used here demonstrates the complexity of this task, where only 738 potential targets are shared between them, representing fewer than half of the genes identified by any one source. We reasoned that the p53 status of the cell lines used would lead to differential expression of p53-regulated genes, and on that basis used DEGs from our data set to select those genes that are identified in at least two of the sources to generate a high confidence list of p53 target genes. These genes show a diverse pattern of expression with some being most strongly expressed in each cell line and some overlap at different levels of expression, so differences in p53 functionality can be appreciated even in resting conditions. The difference in overall p53 activity demonstrates that different mutations in p53 DBD cause varying degrees of loss of function depending on the location of the mutation within the region, in agreement with previous studies[11,18]

The DBD spans amino acids 94-292, with two core domains binding to one half of the DNA element forming a symmetrical dimer with the other two core domains of the tetramer and a small interface between them. Within this domain, R280, mutated in MDA-MB231, is critical because it forms hydrogen bonds with the highly conserved guanine (GGACAT**G**TCC) and with a structural molecule of water as well as with surrounding residues Cys277 and Asp281. It also forms a stabilising salt bridge network with Asp273 to establish sequence-specific contacts in the major groove[10]. The significance of R280 for p53 is confirmed by the sensitivity of this whole region of the protein to alterations in the amino acid sequence, which is consistent with the strongly compromised p53 function in MDA-MB231. This is corroborated by the finding of a variant of p53 lacking residues 257-322 which is incompetent for DNA binding and unable to induce p21[19]. On the other hand, the mutated residue in T47D L194, forms part of the L2 loop of the DBD, that is one of the regions more tolerant to alterations, which is consistent with the milder effect of the T47D mutation on p53 function[20].

DSB of DNA is the strongest threat to genomic integrity and cell survival. It is primarily detected by ATM, which is rapidly activated and phosphorylates MDM2 to stop degradation of p53. ATM can also stabilise p53 by phosphorylation directly or through Chek2 enabling it to induce p21, which will then arrest the cell cycle[21]. Consistent with this mechanism, our data set shows that in MCF-7 and T47D *MDM2* is downregulated in response to DSB suggesting that the pathway to activate p53 by DSB is functional in T47D. In MDA-MB231 *MDM2* and *Chek2* are silenced, testimony of p53 dysfunction since these proteins are part of the p53-feedback regulation. However, ATM can also initiate an immediate phosphorylation cascade that initially targets Chek2 which then phosphorylates Cdcd25A leading to inhibition of cyclin/CDK complexes and causing cell cycle arrest[22,23]. Though Chek1 has long been considered to be the mediator of ATR[24], it can also transmit ATM DNA damage signals[25]. Interestingly, *ATM* and *Chek1* despite being identified as p53 targets, are both upregulated in MDA-MB231, which could arrest the G2/M checkpoint by inhibiting CyclinB/CDK1 via degradation of Cdcd25[26] in a p53-independent fashion.

This would be consistent with the rapid drop in cell density observed in MDA-MB231 MTTA reflecting an arrest of proliferation, as well as the decrease in the proportion of cells in G2/M phase in the recovery time after DNA damage.

The direct control of the cell cycle by p53 occurs at both G1/S and G2/M checkpoints, mainly by up-regulation of CDKN1A/p21 to inhibit the cyclin-dependent kinase (CDK) complexes that drive cell cycle progression. A broad effector of p53, p21 halts the cell cycle by various mechanisms, notably direct interaction with CDK1 and CDK2 or by interference with their phosphorylation[27]. Inhibition of CDK2 prevents phosphorylation of pRB and release of E2F transcription factors, thereby causing the downregulation of key proteins for S-phase progression[9] and arrest at G1. The G2/M checkpoint is controlled by p53 through inhibition of CDK1 (Cdc2) by p21 and also by other p53 targets, *GADD45A* and *GBT2*. Additional p53 targets such as *SFN* (14-3-3δ) can sequester Cdc25 in the cytoplasm preventing activation of cyclin/CDK complexes, and Wee1 that can phosphorylate Cdc2, prevent progression into mitosis and G2/M arrest[15]. Some of these major effectors of p53, namely *CDKN1A* and *BTG2* are downregulated in MDA-MB231 cells, but *GADD45* and *SFN* are upregulated compared to MCF-7 cells, suggesting another pathway of G2/M arrest. The overall higher proportion of cells in G2/M observed in MDA-MB231 cells is consistent with this possibility particularly because these two genes are overexpressed in resting cells as well as treated ones. Interestingly, the T47D cell lines show an expression pattern of these genes, closer to MCF-7, in agreement with its p53 mutation being less damaging for activity, with the exception of p21, that is expressed at intermediate levels between MDA-MB231 and MCF-7. This indicates some impairment in cell cycle arrest in T47D, which corresponds to the higher cell density after treatment with 4NQO observed in MTTAs.

DSB of the DNA is repaired by two main mechanisms, homologous recombination (HR) and Non-Homologous End Joining (NHEJ), but so far participation of p53 in these mechanisms is unclear[28]. HR is most active in S and G2 because of the availability of homologous sister chromatids that can serve as templates, while NHEJ occurs throughout the cell cycle and is therefore the predominant pathway for repair. The role of p53 in HR is mostly independent of its transcriptional activity, through a direct p53 target gene *RAD51* that plays a role in template strand invasion during DNA strand exchange[29]. *RAD51C* is downregulated in MDA-MB231 and T47D indicating that HR is likely to be dysfunctional in these cell lines. The role of p53 in NHEJ seems to be related to p53 exonuclease activity. Interestingly, this activity was found absent in MDA-MB231 compared to MCF-7[30], which is consistent with the exonuclease activity being located in the core region of the protein and therefore reported to be sensitive to mutations in this domain[31]. Some p53 target genes are related to nucleotide excision repair such as *DDB2* and *XPC* as well as other genes with a more general function in repair such as *PCNA* and *POLH*. All these genes are identified on our list of p53 targets and appear severely downregulated in MDA-MB231 cells, consistent with impairment of DNA repair. The low levels of cell death observed in MDA-MB231 imply that the reduced cell density in MTTA is due to cell cycle arrest, yet the effective recovery in the MTTA suggests reset of the cell cycle without repair. This also points to effective cell survival despite a chaotic recovery of the cell cycle is chaotic and high levels of cell death.

In the face of unrepairable DNA damage, cell survival is compromised and cell death occurs, either in a programmed manner by induction of apoptosis or by necrosis due to the inability of the cell to function. Two pathways of apoptosis have been described, the intrinsic type is triggered by cellular stress of the cell while the extrinsic is induced by extracellular signals. In the intrinsic pathway, the sensing of unrepaired DNA damage leads to induction of apoptosis mediators such as BAX, PUMA (BBC3) and NOXA, which cause the release of Cytochrome C from the mitochondria[15]. Once in the cytoplasm, Cytochrome C forms the apoptosome with Apaf-1 and pro-caspase 9, which triggers a cascade of caspase proteases activation that initiates cellular degradation and nuclear condensation. Other p53 targets participate in this process, such as the nuclease AEN and AIFM1, an apoptosis inducer whose regulation by p53 is controversial but we do identify it as a direct p53 target in this study. Expression of *BCL2* and *AIFM1* are strongly downregulated in MDA-MB231 and though less affected in T47D, they are

still markedly reduced. Of note, some of the genes involved in extrinsic apoptosis are also p53-dependent and differentially regulated in the breast cancer cell lines, but not responsive to treatment with 4NQO. It is clear that apoptosis in this study is strongly induced at high concentration and short exposure of 4NQO in MCF-7 and this effect is strongly reduced in the other cell lines. This suggests involvement of p53-dependent and independent pathways, with the p53-dependent on being inactive in both MDA-MB231 and T47D.

Overall, our data shows that specific mutations in the p53 DBD have different effects on its activity. This is consistent with reports of differential effect of mutations in p53, some of which can stimulate spontaneous and damage-induced recombination without affecting G1, for example[28]. Mutations of the MDA-MB231 critical residue impairs DNA repair and apoptosis, but cell cycle arrest in response to DNA damage is maintained through the direct p53-independent pathway of ATM signaling. On the other hand mutations in the more tolerant region as in T47D lead to milder effects as cell cycle arrest and DNA repair seem functional but p53-dependent apoptosis is not. The consequences are that MDA are less prone to death upon DNA damage and able to override cell cycle arrest without repair leading to survival of cells carrying mutations and defects. T47D are much more sensitive to DNA damage, but only to higher levels of damage and seem more efficient at re-setting the cell cycle, which raises the possibility that repair is not fully functional. These findings together with the comprehensive list of direct p53 target genes improve understanding of p53 function and shed light on the physiology of cancer and effects of therapeutic interventions based on DNA damage induction.

REFERENCES

(1) Levine, A. J.; Oren, M. The First 30 Years of P53: Growing Ever More Complex. *Nat Rev Cancer* **2009**, *9* (10), 749–758. https://doi.org/10.1038/nrc2723.

(2) Hernández Borrero, L. J.; El-Deiry, W. S. Tumor Suppressor P53: Biology, Signaling Pathways, and Therapeutic Targeting. *Biochimica et Biophysica Acta (BBA) - Reviews on Cancer* **2021**, *1876* (1), 188556. https://doi.org/10.1016/j.bbcan.2021.188556.

(3) Lane, D. P. Cancer. P53, Guardian of the Genome. *Nature* **1992**, *358* (6381), 15–16. https://doi.org/10.1038/358015a0.

(4) Brown, C. J.; Lain, S.; Verma, C. S.; Fersht, A. R.; Lane, D. P. Awakening Guardian Angels: Drugging the P53 Pathway. *Nat Rev Cancer* **2009**, *9* (12), 862–873. https://doi.org/10.1038/nrc2763.

(5) Bray, F.; Laversanne, M.; Sung, H.; Ferlay, J.; Siegel, R. L.; Soerjomataram, I.; Jemal, A. Global Cancer Statistics 2022: GLOBOCAN Estimates of Incidence and Mortality Worldwide for 36 Cancers in 185 Countries. *CA Cancer J Clin* **2024**, *74* (3), 229–263. https://doi.org/10.3322/caac.21834.

(6) Markowska, A.; Antoszczak, M.; Markowska, J.; Huczyński, A. Gynotoxic Effects of Chemotherapy and Potential Protective Mechanisms. *Cancers (Basel)* **2024**, *16* (12), 2288. https://doi.org/10.3390/cancers16122288.

(7) Lakin, N. D.; Jackson, S. P. Regulation of P53 in Response to DNA Damage. *Oncogene* **1999**, *18* (53), 7644–7655. https://doi.org/10.1038/sj.onc.1203015.

(8) Abuetabh, Y.; Wu, H. H.; Chai, C.; Al Yousef, H.; Persad, S.; Sergi, C. M.; Leng, R. DNA Damage Response Revisited: The P53 Family and Its Regulators Provide Endless Cancer Therapy Opportunities. *Exp Mol Med* **2022**, *54* (10), 1658–1669. https://doi.org/10.1038/s12276-022-00863-4.

(9) Engeland, K. Cell Cycle Regulation: P53-P21-RB Signaling. *Cell Death Differ* **2022**, *29* (5), 946–960. https://doi.org/10.1038/s41418-022-00988-z.

(10) Joerger, A. C.; Fersht, A. R. The Tumor Suppressor P53: From Structures to Drug Discovery. *Cold Spring Harb Perspect Biol* **2010**, *2* (6), a000919. https://doi.org/10.1101/cshperspect.a000919.

(11) Kotler, E.; Shani, O.; Goldfeld, G.; Lotan-Pompan, M.; Tarcic, O.; Gershoni, A.; Hopf, T. A.; Marks, D. S.; Oren, M.; Segal, E. A Systematic P53 Mutation Library Links Differential Functional Impact to Cancer Mutation Pattern and Evolutionary Conservation. *Mol Cell* **2018**, *71* (1), 178-190.e8. https://doi.org/10.1016/j.molcel.2018.06.012.

(12) Bairoch, A. The Cellosaurus, a Cell-Line Knowledge Resource. *J Biomol Tech* **2018**, *29* (2), 25–38. https://doi.org/10.7171/jbt.18-2902-002.

(13) Tate, J. G.; Bamford, S.; Jubb, H. C.; Sondka, Z.; Beare, D. M.; Bindal, N.; Boutselakis, H.; Cole, C. G.; Creatore, C.; Dawson, E.; Fish, P.; Harsha, B.; Hathaway, C.; Jupe, S. C.; Kok, C. Y.; Noble, K.; Ponting, L.; Ramshaw, C. C.; Rye, C. E.; Speedy, H. E.; Stefancsik, R.; Thompson, S. L.; Wang, S.; Ward, S.; Campbell, P. J.; Forbes, S. A. COSMIC: The Catalogue Of Somatic Mutations In Cancer. *Nucleic Acids Res* **2019**, *47* (D1), D941–D947. https://doi.org/10.1093/nar/gky1015.

(14) Zou, Z.; Ohta, T.; Oki, S. ChIP-Atlas 3.0: A Data-Mining Suite to Explore Chromosome Architecture Together with Large-Scale Regulome Data. *Nucleic Acids Res* **2024**, *52* (W1), W45–W53. https://doi.org/10.1093/nar/gkae358.

(15) Fischer, M. Census and Evaluation of P53 Target Genes. *Oncogene* **2017**, *36* (28), 3943–3956. https://doi.org/10.1038/onc.2016.502.

(16) Garcia-Alonso, L.; Holland, C. H.; Ibrahim, M. M.; Turei, D.; Saez-Rodriguez, J. Benchmark and Integration of Resources for the Estimation of Human Transcription Factor Activities. *Genome Res* **2019**, *29* (8), 1363–1375. https://doi.org/10.1101/gr.240663.118.

(17) Milacic, M.; Beavers, D.; Conley, P.; Gong, C.; Gillespie, M.; Griss, J.; Haw, R.; Jassal, B.; Matthews, L.; May, B.; Petryszak, R.; Ragueneau, E.; Rothfels, K.; Sevilla, C.; Shamovsky, V.; Stephan, R.; Tiwari, K.; Varusai, T.; Weiser, J.; Wright, A.; Wu, G.; Stein, L.; Hermjakob, H.; D'Eustachio, P. The Reactome Pathway Knowledgebase 2024. *Nucleic Acids Res* **2024**, *52* (D1), D672–D678. https://doi.org/10.1093/nar/gkad1025.

(18) Sampath, J.; Sun, D.; Kidd, V. J.; Grenet, J.; Gandhi, A.; Shapiro, L. H.; Wang, Q.; Zambetti, G. P.; Schuetz, J. D. Mutant P53 Cooperates with ETS and Selectively Up-Regulates Human MDR1 Not MRP1. *J Biol Chem* **2001**, *276* (42), 39359–39367. https://doi.org/10.1074/jbc.M103429200.

(19) García-Alai, M. M.; Tidow, H.; Natan, E.; Townsley, F. M.; Veprintsev, D. B.; Fersht, A. R. The Novel P53 Isoform "Delta P53" Is a Misfolded Protein and Does Not Bind the P21 Promoter Site. *Protein Sci* **2008**, *17* (10), 1671–1678. https://doi.org/10.1110/ps.036996.108.

(20) Kotler, E.; Shani, O.; Goldfeld, G.; Lotan-Pompan, M.; Tarcic, O.; Gershoni, A.; Hopf, T. A.; Marks, D. S.; Oren, M.; Segal, E. A Systematic P53 Mutation Library Links Differential Functional Impact to Cancer Mutation Pattern and Evolutionary Conservation. *Mol Cell* **2018**, *71* (1), 178-190.e8. https://doi.org/10.1016/j.molcel.2018.06.012.

(21) Cheng, Q.; Chen, J. Mechanism of P53 Stabilization by ATM after DNA Damage. *Cell Cycle* **2010**, *9* (3), 472–478. https://doi.org/10.4161/cc.9.3.10556.

(22) Falck, J.; Mailand, N.; Syljuåsen, R. G.; Bartek, J.; Lukas, J. The ATM-Chk2-Cdc25A Checkpoint Pathway Guards against Radioresistant DNA Synthesis. *Nature* **2001**, *410* (6830), 842–847. https://doi.org/10.1038/35071124.

(23) McGowan, C. H.; Russell, P. The DNA Damage Response: Sensing and Signaling. *Curr Opin Cell Biol* **2004**, *16* (6), 629–633. https://doi.org/10.1016/j.ceb.2004.09.005.

(24) Liu, Q.; Guntuku, S.; Cui, X.-S.; Matsuoka, S.; Cortez, D.; Tamai, K.; Luo, G.; Carattini-Rivera, S.; DeMayo, F.; Bradley, A.; Donehower, L. A.; Elledge, S. J. Chk1 Is an Essential Kinase That Is Regulated by Atr and Required for the G $_2$ /M DNA Damage Checkpoint. *Genes Dev* **2000**, *14* (12), 1448–1459. https://doi.org/10.1101/gad.14.12.1448.

(25) Gatei, M.; Sloper, K.; Sörensen, C.; Syljuäsen, R.; Falck, J.; Hobson, K.; Savage, K.; Lukas, J.; Zhou, B.-B.; Bartek, J.; Khanna, K. K. Ataxia-Telangiectasia-Mutated (ATM) and NBS1-Dependent Phosphorylation of Chk1 on Ser-317 in Response to Ionizing Radiation. *Journal of Biological Chemistry* **2003**, *278* (17), 14806–14811. https://doi.org/10.1074/jbc.M210862200.

(26) Xiao, Z.; Chen, Z.; Gunasekera, A. H.; Sowin, T. J.; Rosenberg, S. H.; Fesik, S.; Zhang, H. Chk1 Mediates S and G2 Arrests through Cdc25A Degradation in Response to DNA-Damaging Agents. *J Biol Chem* **2003**, *278* (24), 21767–21773. https://doi.org/10.1074/jbc.M300229200.

(27) Abbas, T.; Dutta, A. P21 in Cancer: Intricate Networks and Multiple Activities. *Nat Rev Cancer* **2009**, *9* (6), 400–414. https://doi.org/10.1038/nrc2657.

(28) Menon, V.; Povirk, L. Involvement of P53 in the Repair of DNA Double Strand Breaks: Multifaceted Roles of P53 in Homologous Recombination Repair (HRR) and Non-Homologous End Joining (NHEJ). *Subcell Biochem* **2014**, *85*, 321–336. https://doi.org/10.1007/978-94-017-9211-0_17.

(29) Williams, A. B.; Schumacher, B. P53 in the DNA-Damage-Repair Process. *Cold Spring Harb Perspect Med* **2016**, *6* (5). https://doi.org/10.1101/cshperspect.a026070.

(30) Lilling, G.; Elena, N.; Sidi, Y.; Bakhanashvili, M. P53-Associated 3'-->5' Exonuclease Activity in Nuclear and Cytoplasmic Compartments of Cells. *Oncogene* **2003**, *22* (2), 233–245. https://doi.org/10.1038/sj.onc.1206111.

(31) Mummenbrauer, T.; Janus, F.; Müller, B.; Wiesmüller, L.; Deppert, W.; Grosse, F. P53 Protein Exhibits 3'-to-5' Exonuclease Activity. *Cell* **1996**, *85* (7), 1089–1099. https://doi.org/10.1016/s0092-8674(00)81309-4.

ACKNOWLEDGEMENTS

Authors are grateful to the technical staff at the School of Life and Medical Sciences for their help and support. Particular recognition is due to Charming Pena and Marios Konstantinidis for help with experimental work and Michael Kilpatrick for data handling.

FIANACIAL SUPPORT

This work was completed with support from the Centre for Mechanisms of Disease and Drug development, University of Hertfordshire GRANT# 11.101336.3367.000